Charged Hadron A_N in Polarized p+p, p+Al, and p+Au collisions at $\sqrt{s_{NN}} = 200$ GeV

Jeongsu Bok[1], Sanghoon Lim[2], Jin Huang[3]

(1) New Mexico State University

(2) Los Alamos National Laboratory

(3) Brookhaven National Laboratory

March 26, 2018

Abstract

This analysis note provides additional information from Ananote 1325 ("Transverse Single Spin Asymmetries of Charged Hadrons at Forward and Backward Rapidity from Polarized p+p and p+Au collisions at $\sqrt{s_{NN}} = 200$ GeV") for PPG 215. p+Al data is included and results are compared at $0.1 < x_F < 0.2$.

Contents

1 Transverse Single Spin Asymmetry

The transverse single spin asymmetry in inclusive h^- and h^+ production have been studied in 3 p_T ($1.25 < p_T < 7.0$ GeV/c) bins and 5 $|x_F|$ ($0.035 < |x_F| < 0.020$) bins for forward and backward rapidity separately. The measured A_N from the hadron track detected in muon spectrometers cannot be compared with theories or results from other experiments directly because there are momentum migration and charge conversion in the detectors and absorbers. Using methods in the Ananote 1325, unfolded A_N's are calculated. In this analysis note, highest x_F bin is $0.1 < x_F < 0.2$ while previous Ananote 1325 had 0.13¡x_F¡0.2. Also, p+Al result is added. The comparison of A_N for positively charged hadron at $0.1 < x_F < 0.2$ are shown eventually.

1.1 Raw A_N in $p + p$

The asymmetries (blue beam, yellow beam and combined) for charged hadrons stopped at MUID Gap2, 3 are listed in Table 1, 2, 3, 4.

Table 1: p_T dependence of A_N^B(Blue Beam), A_N^Y(Yellow Beam) and A_N(Combined) with statistical uncertainty δA_N^{stat} in forward and backward rapidity. ($-$)charged hadron from $p+p$ collision. Unit of A_N is %.

p_T	$x_F > 0$			$x_F < 0$		
(GeV/c)	$A_N^B(10^{-2})$	$A_N^Y(10^{-2})$	$A_N(10^{-2})$	$A_N^B(10^{-2})$	$A_N^Y(10^{-2})$	$A_N(10^{-2})$
(1.25,2.50)	-0.37±0.22	-0.51±0.24	-0.43±0.16	0.07±0.23	0.01±0.22	0.04±0.16
(2.50,3.50)	-1.09±0.61	-0.87±0.68	-0.99±0.46	-0.73±0.67	-0.03±0.63	-0.36±0.46
(3.50,7.00)	-0.59±1.36	1.93±1.49	0.55±1.01	0.53±1.46	1.37±1.40	0.97±1.01

Table 2: p_T dependence of A_N^B(Blue Beam), A_N^Y(Yellow Beam) and A_N(Combined) with statistical uncertainty δA_N^{stat} in forward and backward rapidity. (+) charged hadron from $p + p$ collision. Unit of A_N is %.

p_T	$x_F > 0)$			$x_F < 0$		
(GeV/c)	$A_N^B(10^{-2})$	$A_N^Y(10^{-2})$	$A_N(10^{-2})$	$A_N^B(10^{-2})$	$A_N^Y(10^{-2})$	$A_N(10^{-2})$
(1.25,2.50)	0.49±0.15	0.61±0.17	0.54±0.11	0.11±0.17	0.31±0.15	0.22±0.11
(2.50,3.50)	3.25±0.42	2.11±0.48	2.75±0.32	-0.57±0.47	-0.29±0.43	-0.42±0.32
(3.50,7.00)	3.63±0.93	2.01±1.02	2.90±0.69	0.19±1.00	1.13±0.95	0.68±0.69

Table 3: x_F dependence of A_N^B(Blue Beam), A_N^Y(Yellow Beam) and A_N(Combined) with statistical uncertainty δA_N^{stat}. $(-)$charged hadron from $p+p$ collision. Unit of A_N is %.

x_F	$A_N^B(10^{-2})$	$A_N^Y(10^{-2})$	$A_N(10^{-2})$
(-0.20,-0.10)	-0.43±0.91	0.73±0.56	0.41±0.48
(-0.10,-0.07)	0.25±0.48	0.05±0.36	0.12±0.28
(-0.07,-0.05)	-0.05±0.34	-0.05±0.35	-0.05±0.24
(-0.05,-0.035)	-0.05±0.38	-0.39±0.51	-0.17±0.31
(0.035,0.05)	0.33±0.49	-0.01±0.39	0.12±0.31
(0.05,0.07)	-0.17±0.34	-0.45±0.34	-0.31±0.24
(0.07,0.10)	-1.01±0.35	-1.37±0.49	-1.13±0.28
(0.10,0.20)	-0.79±0.55	-0.25±0.93	-0.65±0.47

Table 4: x_F dependence of A_N^B(Blue Beam), A_N^Y(Yellow Beam) and A_N(Combined) with statistical uncertainty δA_N^{stat}. $(+)$charged hadron from $p+p$ collision. Unit of A_N is %.

x_F	$A_N^B(10^{-2})$	$A_N^Y(10^{-2})$	$A_N(10^{-2})$
(-0.20,-0.10)	-0.73±0.63	0.07±0.39	-0.15±0.33
(-0.10,-0.07)	-0.11±0.34	0.41±0.25	0.23±0.20
(-0.07,-0.05)	0.09±0.24	0.35±0.24	0.22±0.17
(-0.05,-0.035)	0.23±0.29	-0.11±0.37	0.10±0.23
(0.035,0.05)	-0.27±0.36	0.67±0.30	0.28±0.23
(0.05,0.07)	0.55±0.23	0.55±0.25	0.55±0.17
(0.07,0.10)	0.87±0.24	0.97±0.35	0.90±0.20
(0.10,0.20)	2.99±0.38	2.79±0.65	2.94±0.33

1.2 Raw A_N in p+Au

The asymmetries (blue beam) for charged hadrons stopped at MUID Gap2,3 are listed in Table 5, 6.

Table 5: p_T dependence of A_N(Blue Beam) with statistical uncertainty δA_N^{stat} in p+Au collision

p_T (GeV/c)	p+Au 0-84% $A_N(10^{-2})$	p+Au 0-20% $A_N(10^{-2})$	p+Au 20-50% $A_N(10^{-2})$	p+Au 50-84% $A_N(10^{-2})$
(-)chg. $x_F > 0$				
(1.25,2.50)	-0.39±0.31	-0.93±0.53	0.43±0.49	-0.79±0.59
(2.50,3.50)	-0.31±0.74	0.23±1.27	0.09±1.17	-1.39±1.46
(3.50,7.00)	0.53±1.53	1.57±2.64	0.81±2.41	-1.59±2.9
(-)chg. $x_F < 0$				
(1.25,2.50)	-0.11±0.25	-0.37±0.35	0.41±0.41	-0.35±0.62
(2.50,3.50)	-0.41±0.75	-0.67±1.08	0.13±1.24	-0.09±1.86
(3.50,7.00)	0.33±1.62	2.63±2.38	-3.81±2.65	2.81±3.95
(+)chg. $x_F > 0$				
(1.25,2.50)	0.25±0.22	0.17±0.37	0.03±0.34	0.63±0.42
(2.50,3.50)	0.07±0.51	0.33±0.87	-0.67±0.81	0.55±1.00
(3.50,7.00)	1.17±1.05	0.19±1.81	0.81±1.66	3.11±2.05
(+)chg. $x_F < 0$				
(1.25,2.50)	0.27±0.21	0.31±0.30	0.09±0.36	0.51±0.53
(2.50,3.50)	-0.09±0.58	0.25±0.83	-0.51±0.96	0.33±1.48
(3.50,7.00)	-1.07±1.23	-1.49±1.80	-1.29±2.03	0.85±3.07

Table 6: x_F dependence of A_N(Blue Beam) with statistical uncertainty δA_N^{stat} in p+Au collision

x_F	p+Au 0-84% $A_N(10^{-2})$	p+Au 0-20% $A_N(10^{-2})$	p+Au 20-50% $A_N(10^{-2})$	p+Au 50-84% $A_N(10^{-2})$
(-)chg. $x_F > 0$				
(0.035,0.050)	-0.57±0.81	-1.57±1.28	2.25±1.21	-2.77±1.49
(0.050,0.070)	-0.31±0.52	-1.09±0.84	-0.09±0.78	-0.45±0.94
(0.070,0.100)	0.03±0.50	-0.55±0.81	0.33±0.74	-0.33±0.90
(0.100,0.200)	-0.05±0.71	0.63±1.16	-0.05±1.06	-1.53±1.30
(-)chg. $x_F < 0$				
(-0.035,-0.050)	0.05±0.38	-0.53±0.51	0.31±0.59	0.57±0.87
(-0.050,-0.070)	-0.27±0.41	-0.63±0.55	0.55±0.64	-1.57±0.96
(-0.070,-0.100)	-0.05±0.62	0.09±0.84	0.31±0.97	0.23±1.47
(-0.100,-0.200)	0.55±1.15	2.17±1.57	-1.81±1.82	0.69±2.75
(+)chg. $x_F > 0$				
(0.035,0.050)	0.27±0.58	0.39±0.92	-0.89±0.87	1.51±1.07
(0.050,0.070)	0.05±0.36	0.21±0.58	0.13±0.54	-0.47±0.65
(0.070,0.100)	0.51±0.35	0.61±0.56	0.09±0.52	1.07±0.63
(0.100,0.200)	0.31±0.50	-0.85±0.81	-0.05±0.74	1.57±0.90
(+)chg. $x_F < 0$				
(-0.035,-0.050)	0.27±0.34	0.37±0.45	0.25±0.54	-0.27±0.80
(-0.050,-0.070)	-0.07±0.33	-0.21±0.45	-0.13±0.53	0.17±0.80
(-0.070,-0.100)	0.81±0.48	0.49±0.65	0.09±0.76	2.47±1.17
(-0.100,-0.200)	0.49±0.88	1.93±1.19	-1.35±1.39	1.69±2.13

1.3 Raw A_N in p+Al

The asymmetries (blue beam) for charged hadrons stopped at MUID Gap2,3 are listed in Table 7, 8. Cuts are same as p+Au's one except for maximum centrality cut 72%.

Table 7: p_T dependence of A_N(Blue Beam) with statistical uncertainty δA_N^{stat} in p+Al collision

p_T (GeV/c)	p+Al 0-72% $A_N(10^{-2})$	p+Al 0-40% $A_N(10^{-2})$	p+Al 40-72% $A_N(10^{-2})$
(-)chg. $x_F > 0$			
(1.25,2.50)	-0.61±0.39	-0.35±0.46	-0.83±0.67
(2.50,3.50)	-0.41±0.99	-1.25±1.18	0.41±1.74
(3.50,5.00)	-0.85±2.12	-0.81±2.52	-1.57±3.72
(-)chg. $x_F < 0$			
(1.25,2.50)	0.29±0.38	0.49±0.43	-0.11±0.77
(2.50,3.50)	-0.21±1.13	0.71±1.28	-1.97±2.28
(3.50,7.00)	1.51±2.45	-1.75±2.81	7.69±4.82
(+)chg. $x_F > 0$			
(1.25,2.50)	0.31±0.27	0.47±0.32	0.17±0.47
(2.50,3.50)	1.53±0.69	0.75±0.82	4.25±1.19
(3.50,7.00)	2.41±1.45	3.33±1.74	1.35±2.51
(+)chg. $x_F < 0$			
(1.25,2.50)	-0.81±0.31	-1.07±0.35	0.29±0.64
(2.50,3.50)	-0.89±0.86	-0.45±0.97	-1.69±1.75
(3.50,7.00)	2.43±1.84	2.89±2.13	4.07±3.59

- Note : K/π ratio in p+Al collisions According to HIJING simulation, the difference of K/π between p+Al and p+Au are smaller than the systematic uncertainty assigned already (±30%) in the region of this analysis ($1.25 < p_T < 7.0$ GeV/c) in Figure 1, same K/π ratio are assumed with the same large systematic uncertainty.

Table 8: x_F dependence of A_N(Blue Beam) with statistical uncertainty δA_N^{stat} in p+Al collision

x_F	p+Al 0-72% $A_N(10^{-2})$	p+Al 0-40% $A_N(10^{-2})$	p+Al 40-72% $A_N(10^{-2})$
(-)chg. $x_F > 0$			
(0.035,0.050)	-0.95±0.91	0.03±1.08	-2.83±1.61
(0.050,0.070)	-0.73±0.61	-0.61±0.72	-0.65±1.06
(0.070,0.100)	-0.53±0.60	-0.57±0.71	-0.49±1.05
(0.100,0.200)	-0.07±0.90	-0.51±1.07	0.71±1.55
(-)chg. $x_F < 0$			
(-0.035,-0.050)	0.57±0.56	0.61±0.64	0.35±1.13
(-0.050,-0.070)	-0.39±0.58	-0.05±0.66	-0.63±1.19
(-0.070,-0.100)	0.33±0.86	0.41±0.98	-0.57±1.75
(-0.100,-0.200)	2.89±1.63	3.57±1.85	1.35±3.29
(+)chg. $x_F > 0$			
(0.035,0.050)	0.85±0.66	0.91±0.78	1.27±1.18
(0.050,0.070)	0.05±0.42	0.27±0.50	-0.31±0.74
(0.070,0.100)	0.59±0.42	0.47±0.50	1.15±0.73
(0.100,0.200)	1.21±0.63	1.27±0.75	1.75±1.08
(+)chg. $x_F < 0$			
(-0.035,-0.050)	-0.77±0.48	-0.61±0.55	-1.13±0.98
(-0.050,-0.070)	-1.05±0.46	-1.49±0.52	1.09±0.95
(-0.070,-0.100)	-0.17±0.66	-0.65±0.74	1.31±1.37
(-0.100,-0.200)	-0.43±1.24	0.53±1.42	-1.59±2.49

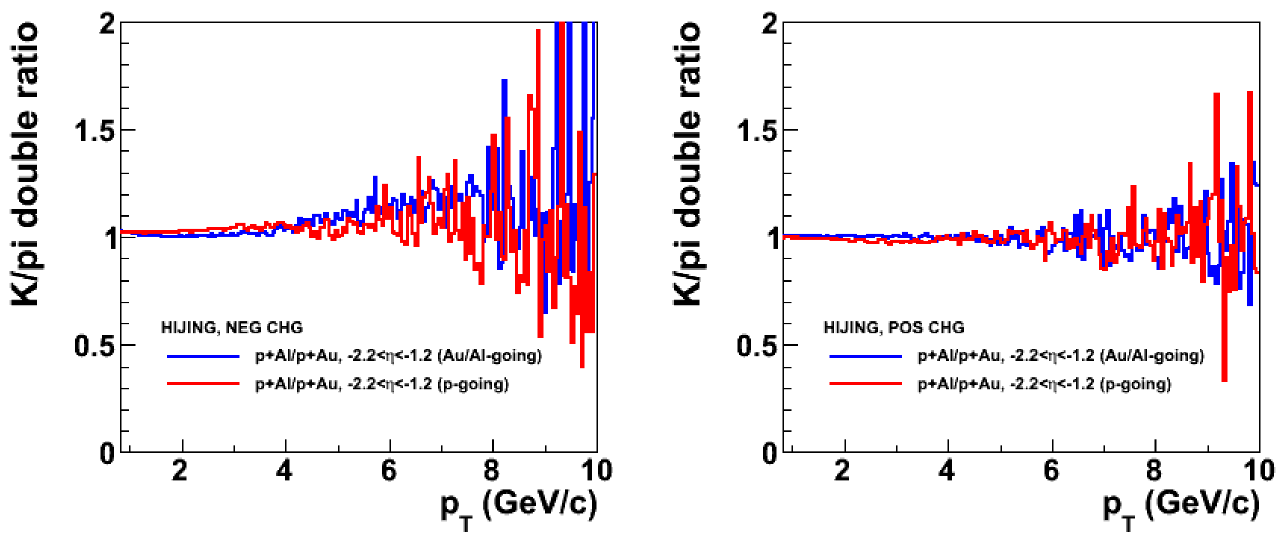

Figure 1: K/π double ratio for comparison between p+Al and p+Au from the HIJING simulation. The difference is much smaller than the original $\delta K/\pi$ relative ±30% in the region of this analysis, $1.25 < p_T < 7.0$ GeV/c.

2 Unfolded result

Momentum migration effect was studied in Ananote 1325. Also, the possible change in the migration matrix is considered as a source of systematic uncertainty. Three hadron interaction package in GEANT4 and ±30% variation in K/π ratio are tested. Following figures show raw A_N, unfolded A_N, and systematic effect from the modification of the migration matrix caused by hadron interaction packages and K/π variation in Figure 2, 3. The effects from both systematic variation are turned out to be very small compared to other sources of systematic uncertainty which will be shown in following chapters.

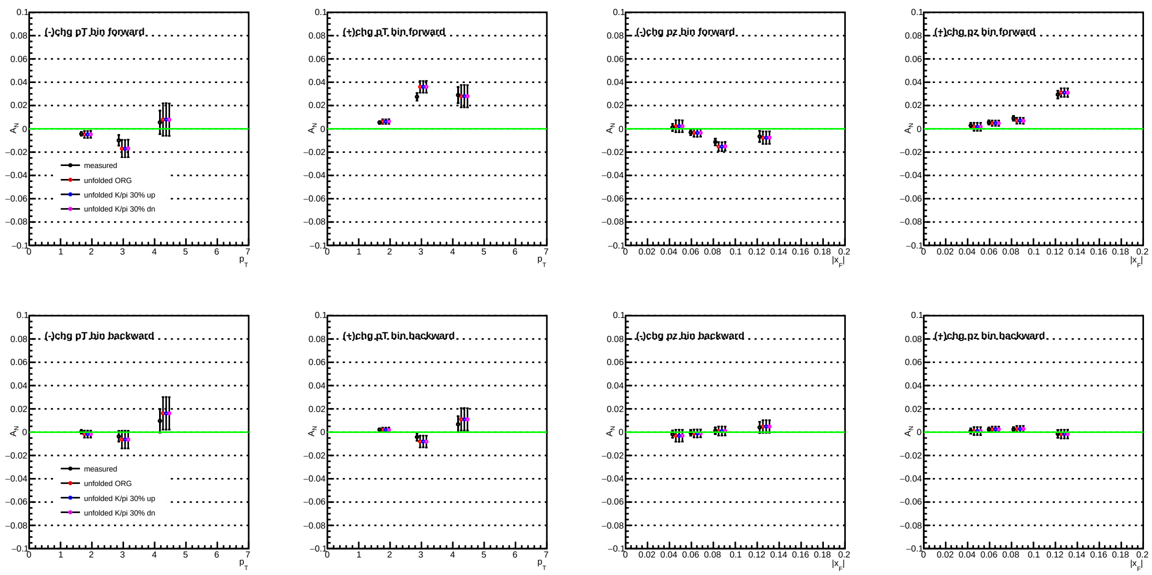

Figure 2: Unfolded A_N in $p+p$ with changing K/π ratio by ±30%. The difference is included in the systematic uncertainty.

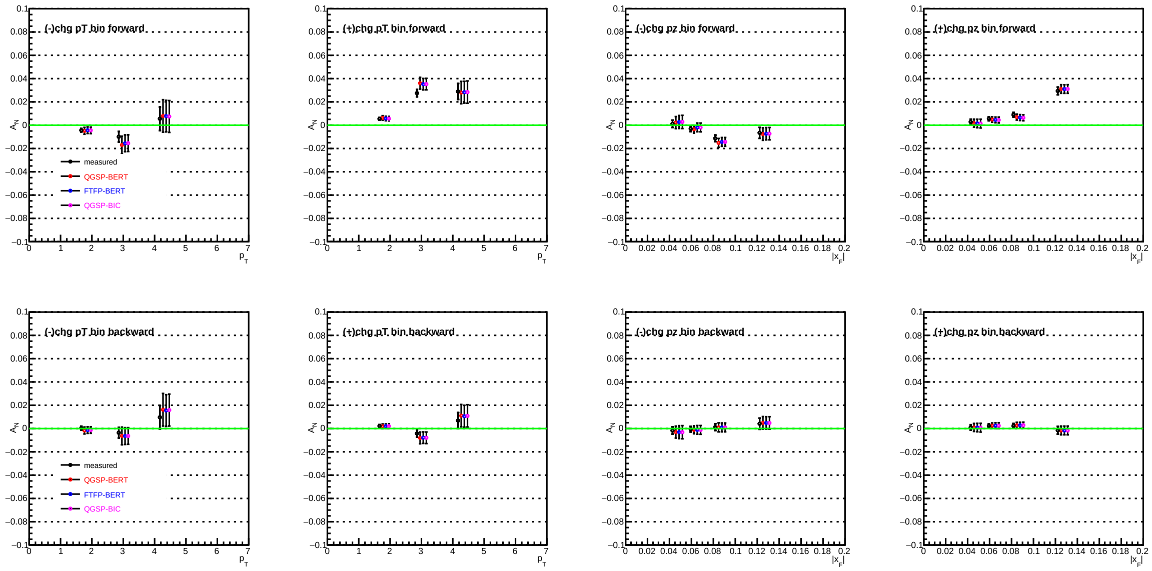

Figure 3: Unfolded A_N in $p + p$ with changing hadron interaction packages. The difference is included in the systematic uncertainty.

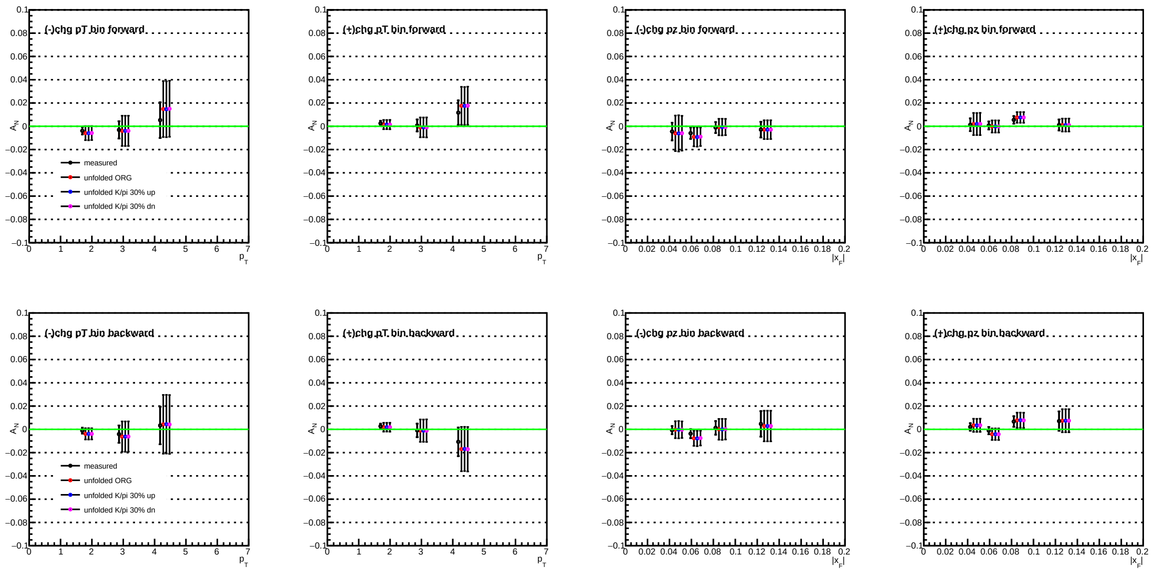

Figure 4: Unfolded A_N in p+Au (0-84%) with changing K/π ratio by $\pm$30%. The difference is included in the systematic uncertainty.

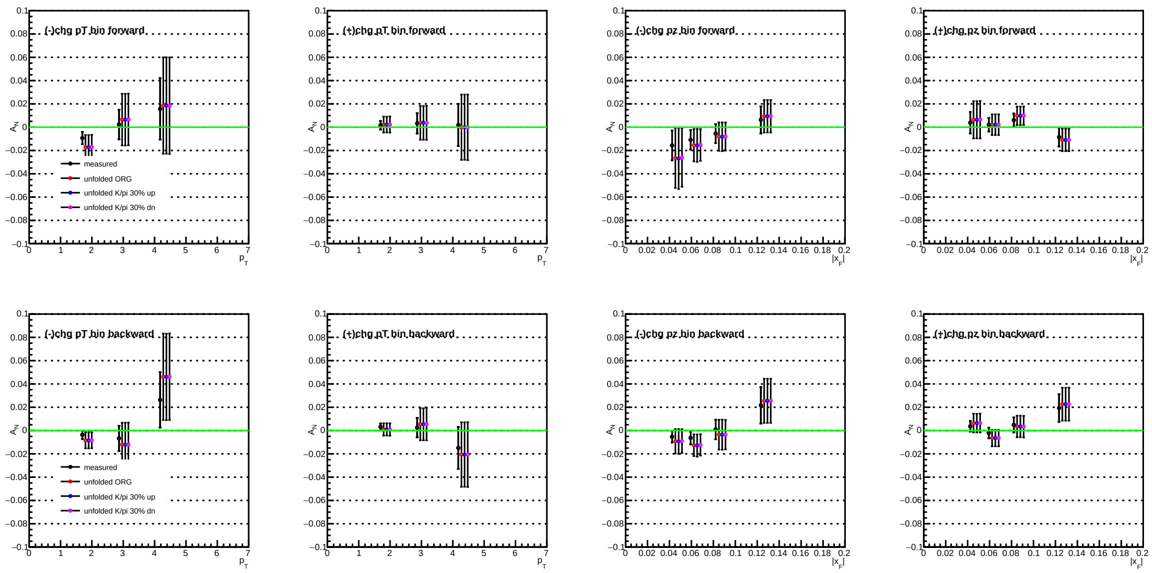

Figure 5: Unfolded A_N in p+Au (0-20%) with changing K/π ratio by $\pm$30%. The difference is included in the systematic uncertainty.

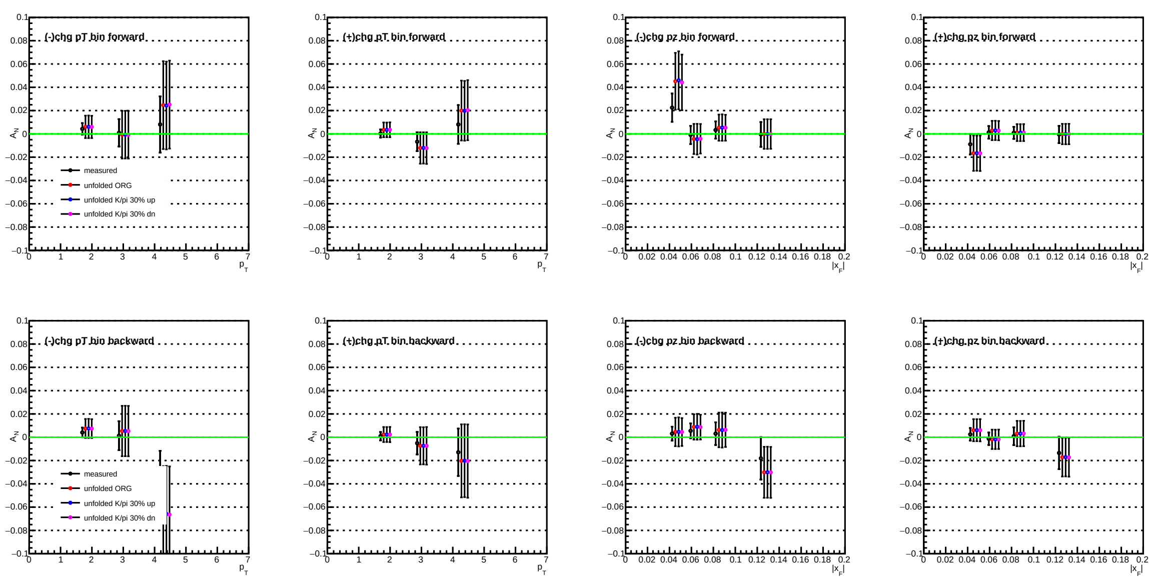

Figure 6: Unfolded A_N in p+Au (20-50%) with changing K/π ratio by $\pm$30%. The difference is included in the systematic uncertainty.

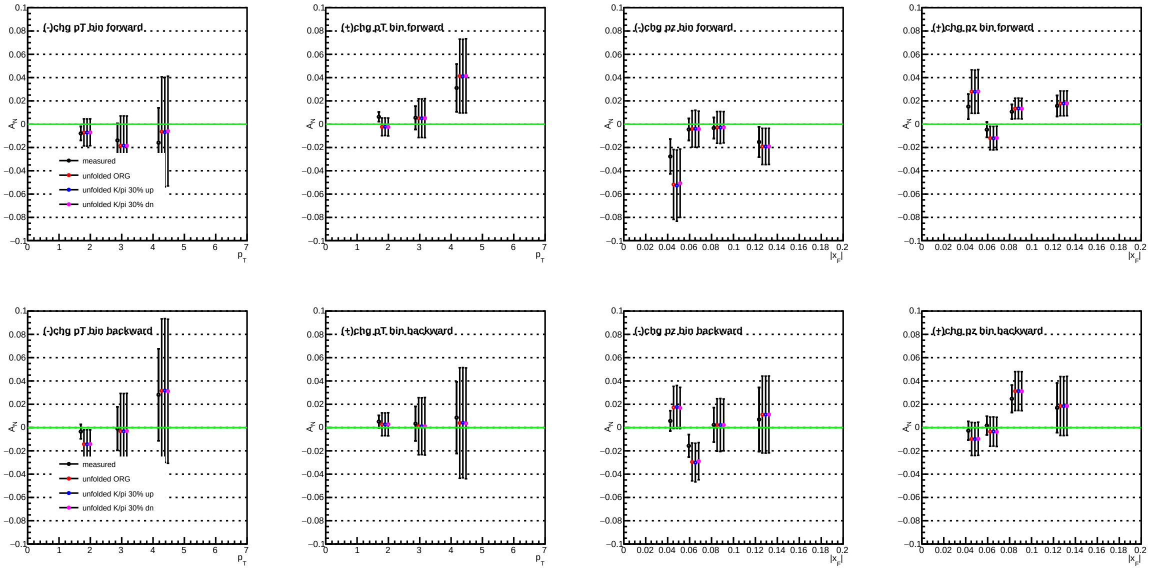

Figure 7: Unfolded A_N in p+Au (50-84%) with changing K/π ratio by $\pm$30%. The difference is included in the systematic uncertainty.

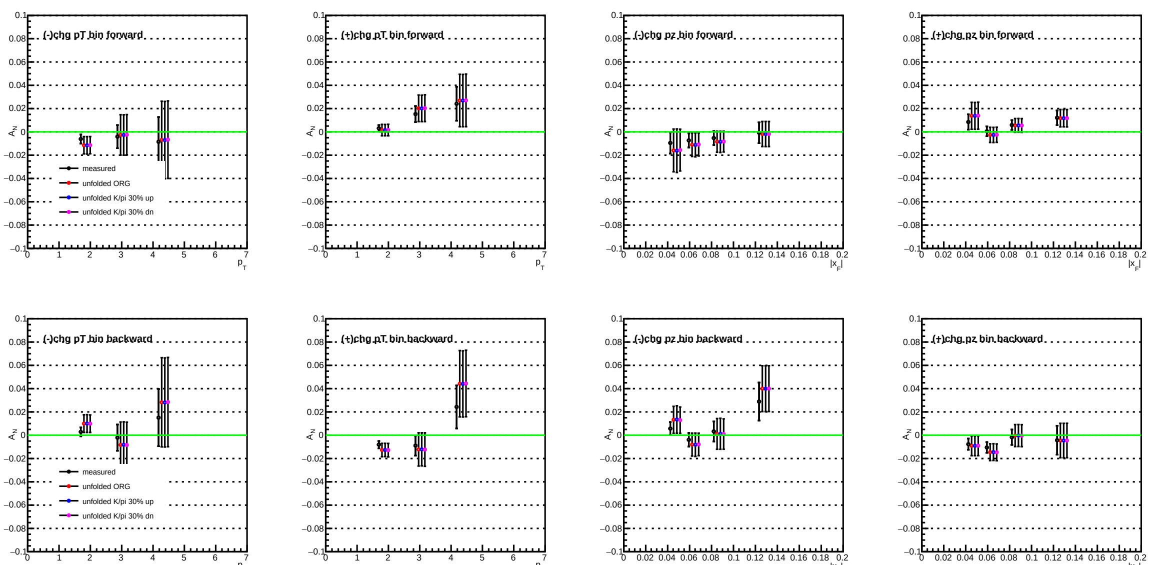

Figure 8: Unfolded A_N in p+Al (0-72%) with changing K/π ratio by $\pm$30%. The difference is included in the systematic uncertainty.

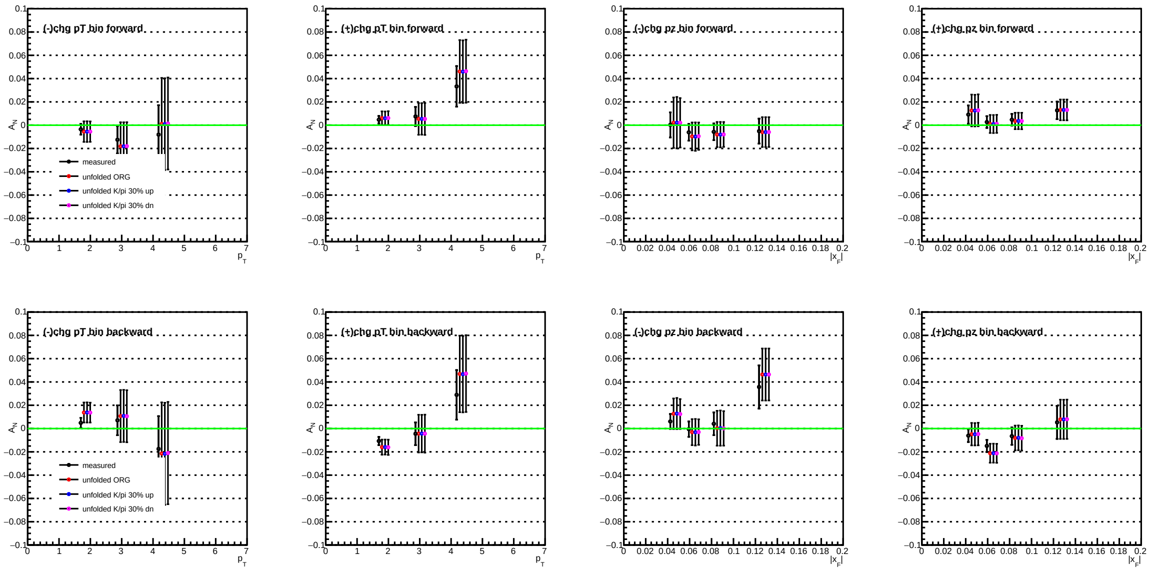

Figure 9: Unfolded A_N in p+Al (0-40%) with changing K/π ratio by $\pm$30%. The difference is included in the systematic uncertainty.

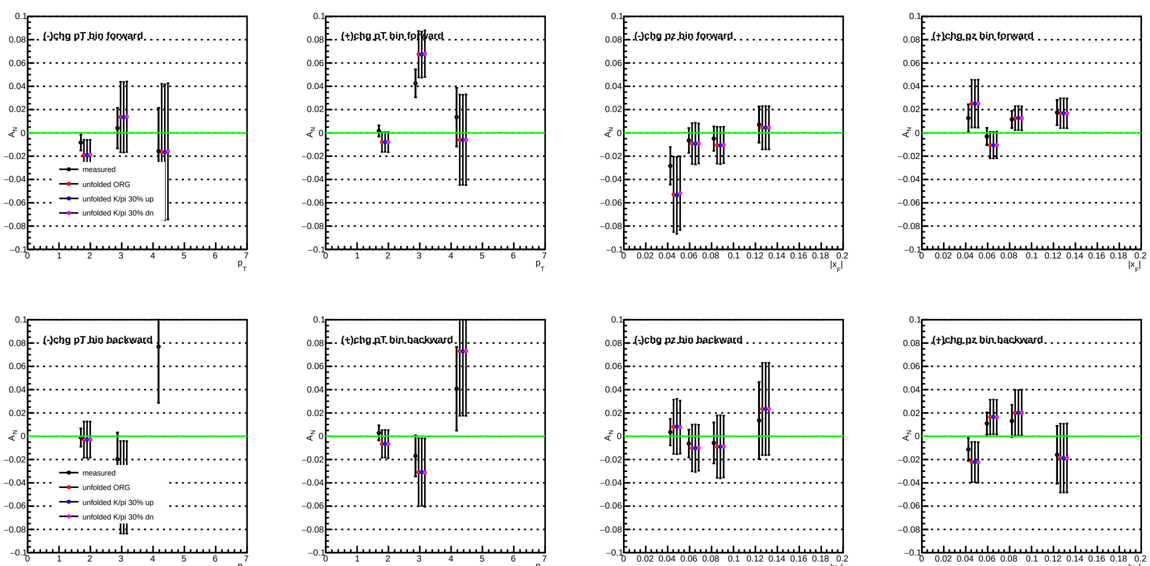

Figure 10: Unfolded A_N in p+Al (41-72%) with changing K/π ratio by $\pm$30%. The difference is included in the systematic uncertainty.

3 Systematic uncertainty

Systematic Uncertainties and unfolded A_N are listed in this section. Section 3.4 describes additional systematic uncertainty assigned in this analysis while others are same as already studied in the Ananote 1325.

3.1 Analysis Method

The difference of result between Maximum Likelihood method and Cosine fit method is assigned as a source of systematic uncertainty for all results. It is listed as δA_N^{method} in tables.

3.2 Contribution from other spices

K^0, p, $\bar{p}$ are included in the hadron cocktail simulation, so we take the asymmetries from those sources in systematic uncertainty (δA_N^{proton}). We assumed that the size of A_N from K^0 is comparable with K^+ and K^-. Based on previous BRAHMS result (PRL 101 042001(2008), AIP Conf. Proc. 915, 533 (2007)), $A_N(p)$, $A_N(\bar{p})$, K^0 are assumed to be smaller than ±0.02. This uncertainty is applied to both forward and backward rapidity ($x_F > 0$) and both $p + p$ and p+Au. It is listed as δA_N^{proton} in tables.

3.3 Uncertainty in the Migration Matrix

We performed hadron cocktail simulation using 3 hadron interaction packages in GEANT4, called QGSP-BERT, FTFP-BERT, QGSP-BIC. These can make different aspects in interactions between particles and material especially in the front absorber located in front of Muon Tracker. For example, momentum migration and charge conversion can be different, so that migration matrix in previous section can be changed. The changes in unfolded A_N caused by different migration matrices in unfolding stage are considered as systematic uncertainty. Also, K/π ratio could affect to the migration matrix, so that it is studied by checking the changes within the variation of K/π ratio by $\pm30\%$ relatively. These uncertainties are smaller than others, included as δA_N^{matrix}.

3.4 Uncertainty from K/π ratio

Even though changes in migration matrix from $\delta K/\pi$ are very small, uncertainty in K/π can cause modification of A_N because charged hadrons include $K^{\pm}$ and $\pi^{\pm}$ which would have different A_N. To compare the results of $p+p$ and $p+A$ directly, possible changes from the uncertainty and difference of K/π ratio are studied based on the models from theory curve provided by Daniel Pitonyak based on the recent paper (PLB770 242-251(2017), arxiv:1512.02252), shown in 12, 12 and BRAHMS data 13. The theory, BRAHMS data, and many π^0 results support a trend of increasing size of A_N for increasing x_F at $x_F > 0$. Also the result of this analysis agrees with that. From the BRAHMS result, two kinds of estimation were made. The first one is theory curve, the other one is estimation from BRAHMS : $A_N(\pi^+) = 0.3 \cdot x_F$, $A_N(\pi^-) = -0.3 \cdot x_F$, and $A_N(K^{\pm}) = 0.15 \cdot x_F$.

With these inputs and hadron cocktail simulation, the weighted sum of A_N of K, π mixture is obtained. Then it is possible to quantify the effect from $\pm 30\% \delta K/\pi$ variation or hadron interaction packages by checking variation of A_N for each case. The systematic uncertainty for $p+p$ result is calculated by the quadrature sum of (1)largest deviation of A_N for other two hadron interaction packages and (2)$\pm 30\%$ variation of K/π. Among two models, the larger variation was chosen as a conservative systematic uncertainty. For p+Au and p+Al, same procedure and same models are used, with hadron cocktail simulation for p+Au which had different K/π ratio from $p+p$. Then, the similar quadrature sum of (1),(2) was made. However, we picked the deviation from the A_N mixture of $p+p$ simulation if it is larger than (2)$\pm 30\%$ variation of K/π. Then this systematic uncertainty covers the difference of K/π in $p+p$, $p+Al$, $p+Au$, and finally the results become comparable each other in the same plot. The calculation is shown in Figure 14. Like other sources of systematic uncertainty, same uncertainty is applied to the result of centrality binning for the same dataset (p+Au or p+Al) based on the description in PHENIX PPG146 (PhysRevC.88.024906) : K/π ratios are essentially identical for all centrality classes.

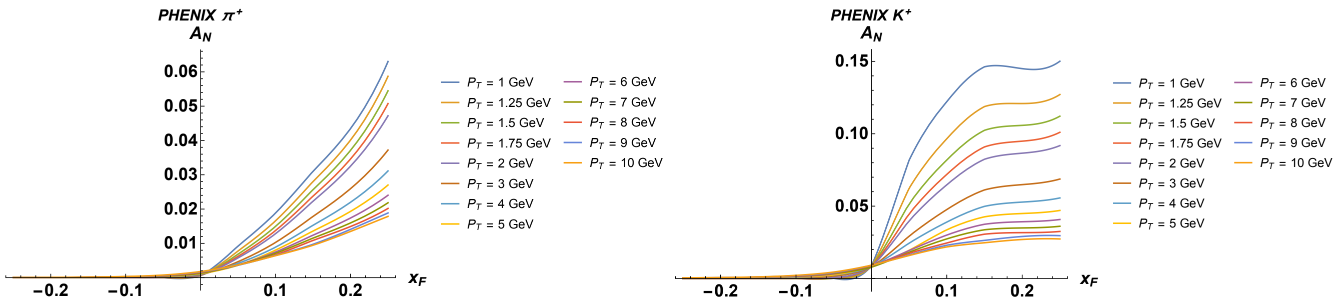

Figure 11: Theory prediction for $A_N(\pi^+)$ and $A_N(K^+)$ in $1.2 < |\eta| < 2.4$

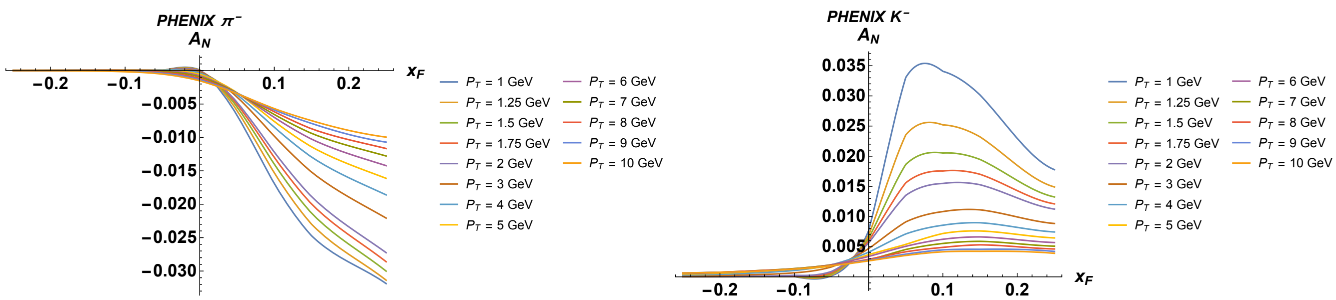

Figure 12: Theory prediction for $A_N(\pi^-)$ and $A_N(K^-)$ in $1.2 < |\eta| < 2.4$

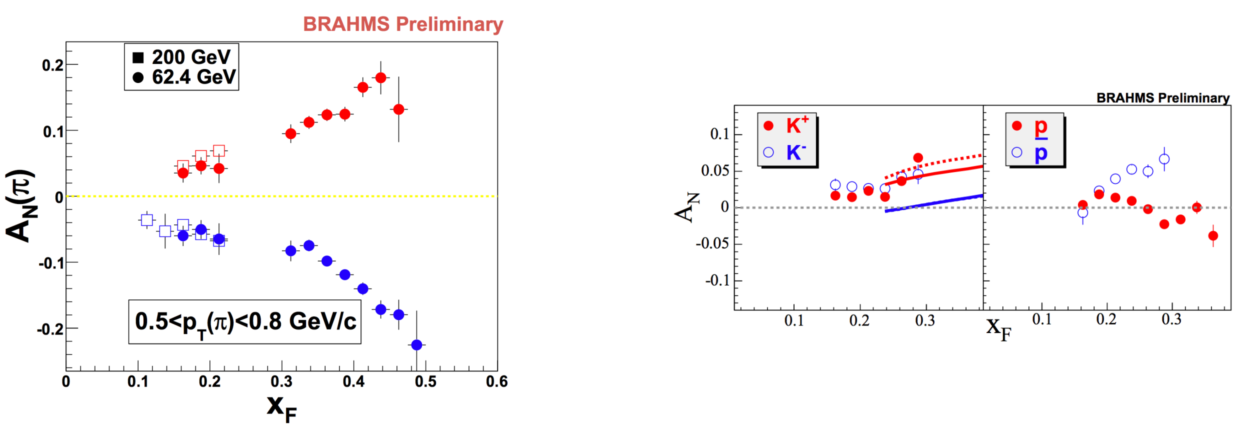

Figure 13: Previous BRAHMS result at forward rapidity.

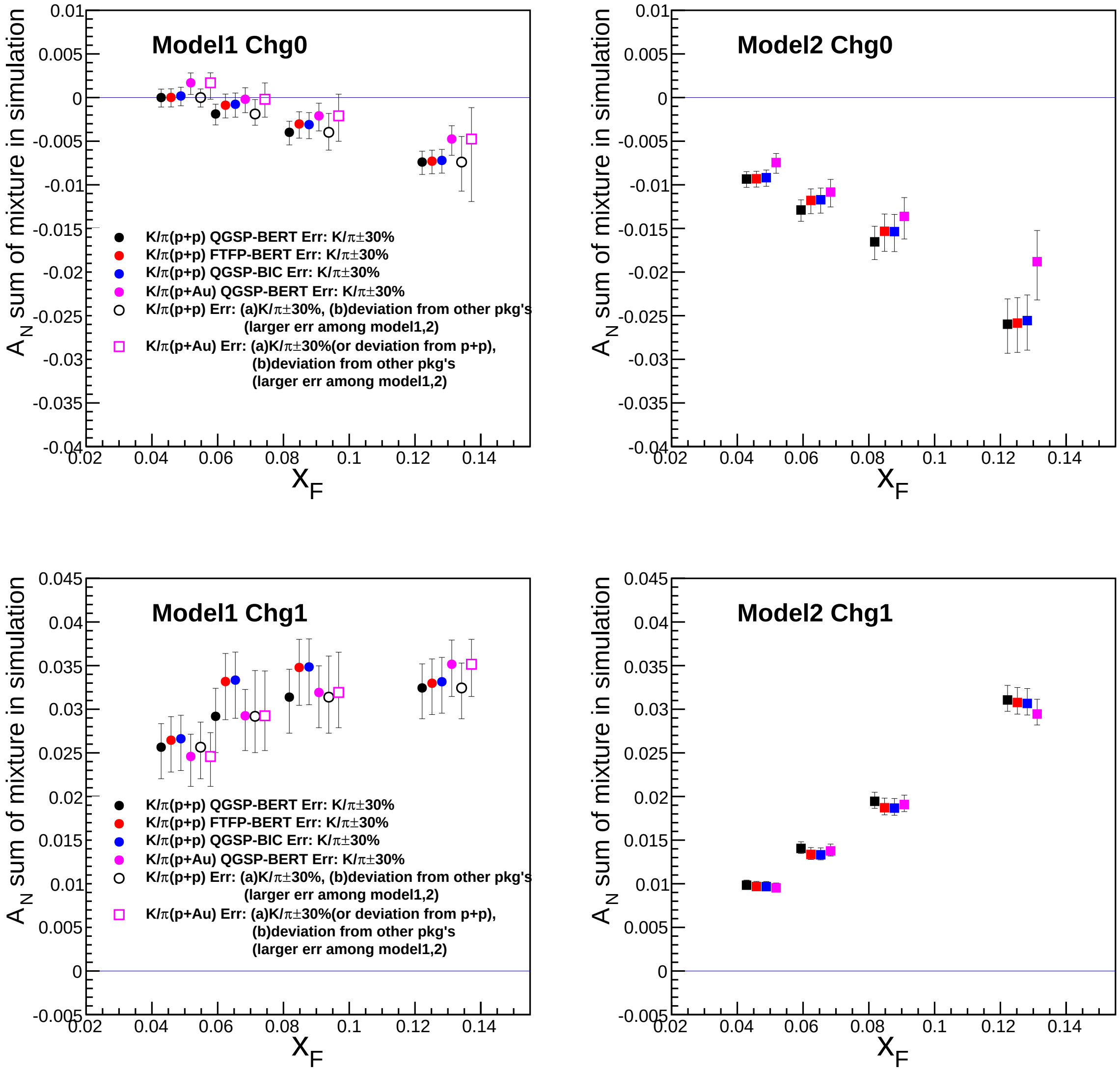

Figure 14: $A_N(mixture)$ are obtained for 2 models (1)theory curve from Daniel Pitonyak(PLB770 242-251(2017)),(2) linear extrapolation from BRAHMS results, using hadron cocktail simulation for $p+p$, p+Au(Al). The error bars of filled circles came from varying K/π by 30%. The error bar on the open circle shows the final systematic uncertainty for $p+p$. It is calculated by quadrature sum of error from K/π variation and hadron interaction packages. The open square is the uncertainty of p+Au(Al) case. The procedure is same, but (2) is replaced as the difference between $A_N(p+p)$(mixture) and $A_N(p+A)$(mixture) when it is larger than (2). This allows a direct comparison between $p+p$, p+Al, and p+Au because K/π difference is covered by this systematic uncertainty.

.

3.5 Tables of systematic uncertainty

Following tables will list each source of systematic uncertainty and total systematic uncertainty for x_F bins.

Table 9: Systematic uncertainty of unfolded A_N for x_F bin in p+p

(-)chg.					
x_F	$\delta A_N^{syst.}$	δA_N^{method}	δA_N^{proton}	δA_N^{matrix}	$\delta A_N^{K/\pi}$
(-0.200,-0.100)	$^{+0.10}_{-0.07} \times 10^{-2}$	$^{+0.06}_{-0.06} \times 10^{-2}$	$^{+0.04}_{-0.04} \times 10^{-2}$	$^{+0.07}_{-0.00} \times 10^{-2}$	$^{+0.00}_{-0.00} \times 10^{-2}$
(-0.100,-0.070)	$^{+0.04}_{-0.04} \times 10^{-2}$	$^{+0.02}_{-0.02} \times 10^{-2}$	$^{+0.03}_{-0.03} \times 10^{-2}$	$^{+0.00}_{-0.02} \times 10^{-2}$	$^{+0.00}_{-0.00} \times 10^{-2}$
(-0.070,-0.050)	$^{+0.03}_{-0.07} \times 10^{-2}$	$^{+0.01}_{-0.01} \times 10^{-2}$	$^{+0.03}_{-0.03} \times 10^{-2}$	$^{+0.00}_{-0.06} \times 10^{-2}$	$^{+0.00}_{-0.00} \times 10^{-2}$
(-0.050,-0.035)	$^{+0.07}_{-0.15} \times 10^{-2}$	$^{+0.06}_{-0.06} \times 10^{-2}$	$^{+0.03}_{-0.03} \times 10^{-2}$	$^{+0.00}_{-0.13} \times 10^{-2}$	$^{+0.00}_{-0.00} \times 10^{-2}$
(-0.035,0.050)	$^{+0.16}_{-0.13} \times 10^{-2}$	$^{+0.04}_{-0.04} \times 10^{-2}$	$^{+0.06}_{-0.06} \times 10^{-2}$	$^{+0.10}_{-0.01} \times 10^{-2}$	$^{+0.10}_{-0.11} \times 10^{-2}$
(0.050,0.070)	$^{+0.18}_{-0.15} \times 10^{-2}$	$^{+0.02}_{-0.02} \times 10^{-2}$	$^{+0.06}_{-0.06} \times 10^{-2}$	$^{+0.01}_{-0.04} \times 10^{-2}$	$^{+0.16}_{-0.13} \times 10^{-2}$
(0.070,0.100)	$^{+0.23}_{-0.45} \times 10^{-2}$	$^{+0.06}_{-0.06} \times 10^{-2}$	$^{+0.06}_{-0.06} \times 10^{-2}$	$^{+0.02}_{-0.39} \times 10^{-2}$	$^{+0.22}_{-0.20} \times 10^{-2}$
(0.100,0.200)	$^{+0.30}_{-0.36} \times 10^{-2}$	$^{+0.03}_{-0.03} \times 10^{-2}$	$^{+0.07}_{-0.07} \times 10^{-2}$	$^{+0.01}_{-0.11} \times 10^{-2}$	$^{+0.29}_{-0.33} \times 10^{-2}$
(+)chg.					
(-0.200,-0.100)	$^{+0.14}_{-0.15} \times 10^{-2}$	$^{+0.09}_{-0.09} \times 10^{-2}$	$^{+0.11}_{-0.11} \times 10^{-2}$	$^{+0.00}_{-0.02} \times 10^{-2}$	$^{+0.00}_{-0.00} \times 10^{-2}$
(-0.100,-0.070)	$^{+0.13}_{-0.12} \times 10^{-2}$	$^{+0.04}_{-0.04} \times 10^{-2}$	$^{+0.11}_{-0.11} \times 10^{-2}$	$^{+0.05}_{-0.00} \times 10^{-2}$	$^{+0.00}_{-0.00} \times 10^{-2}$
(-0.070,-0.050)	$^{+0.10}_{-0.10} \times 10^{-2}$	$^{+0.05}_{-0.05} \times 10^{-2}$	$^{+0.08}_{-0.08} \times 10^{-2}$	$^{+0.03}_{-0.00} \times 10^{-2}$	$^{+0.00}_{-0.00} \times 10^{-2}$
(-0.050,-0.035)	$^{+0.08}_{-0.08} \times 10^{-2}$	$^{+0.03}_{-0.03} \times 10^{-2}$	$^{+0.07}_{-0.07} \times 10^{-2}$	$^{+0.00}_{-0.00} \times 10^{-2}$	$^{+0.00}_{-0.00} \times 10^{-2}$
(-0.035,0.050)	$^{+0.34}_{-0.42} \times 10^{-2}$	$^{+0.03}_{-0.03} \times 10^{-2}$	$^{+0.18}_{-0.18} \times 10^{-2}$	$^{+0.00}_{-0.11} \times 10^{-2}$	$^{+0.29}_{-0.36} \times 10^{-2}$
(0.050,0.070)	$^{+0.56}_{-0.46} \times 10^{-2}$	$^{+0.02}_{-0.02} \times 10^{-2}$	$^{+0.18}_{-0.18} \times 10^{-2}$	$^{+0.00}_{-0.07} \times 10^{-2}$	$^{+0.52}_{-0.42} \times 10^{-2}$
(0.070,0.100)	$^{+0.51}_{-0.50} \times 10^{-2}$	$^{+0.04}_{-0.04} \times 10^{-2}$	$^{+0.20}_{-0.20} \times 10^{-2}$	$^{+0.01}_{-0.21} \times 10^{-2}$	$^{+0.47}_{-0.41} \times 10^{-2}$
(0.100,0.200)	$^{+0.37}_{-0.39} \times 10^{-2}$	$^{+0.05}_{-0.05} \times 10^{-2}$	$^{+0.15}_{-0.15} \times 10^{-2}$	$^{+0.17}_{-0.01} \times 10^{-2}$	$^{+0.28}_{-0.35} \times 10^{-2}$

Table 10: Systematic uncertainty of unfolded A_N for x_F bin in p+Au

(-)chg.					
x_F	$\delta A_N^{syst.}$	δA_N^{method}	δA_N^{proton}	δA_N^{matrix}	$\delta A_N^{K/\pi}$
(-0.200,-0.100)	$^{+0.09}_{-0.09} \times 10^{-2}$	$^{+0.01}_{-0.01} \times 10^{-2}$	$^{+0.04}_{-0.04} \times 10^{-2}$	$^{+0.00}_{-0.00} \times 10^{-2}$	$^{+0.00}_{-0.00} \times 10^{-2}$
(-0.100,-0.070)	$^{+0.10}_{-0.10} \times 10^{-2}$	$^{+0.01}_{-0.01} \times 10^{-2}$	$^{+0.03}_{-0.03} \times 10^{-2}$	$^{+0.01}_{-0.01} \times 10^{-2}$	$^{+0.00}_{-0.00} \times 10^{-2}$
(-0.070,-0.050)	$^{+0.10}_{-0.10} \times 10^{-2}$	$^{+0.03}_{-0.03} \times 10^{-2}$	$^{+0.03}_{-0.03} \times 10^{-2}$	$^{+0.02}_{-0.02} \times 10^{-2}$	$^{+0.00}_{-0.00} \times 10^{-2}$
(-0.050,-0.035)	$^{+0.10}_{-0.10} \times 10^{-2}$	$^{+0.02}_{-0.02} \times 10^{-2}$	$^{+0.03}_{-0.03} \times 10^{-2}$	$^{+0.00}_{-0.00} \times 10^{-2}$	$^{+0.00}_{-0.00} \times 10^{-2}$
(-0.035,0.050)	$^{+0.17}_{-0.23} \times 10^{-2}$	$^{+0.02}_{-0.02} \times 10^{-2}$	$^{+0.06}_{-0.06} \times 10^{-2}$	$^{+0.01}_{-0.01} \times 10^{-2}$	$^{+0.11}_{-0.19} \times 10^{-2}$
(0.050,0.070)	$^{+0.22}_{-0.24} \times 10^{-2}$	$^{+0.02}_{-0.02} \times 10^{-2}$	$^{+0.06}_{-0.06} \times 10^{-2}$	$^{+0.01}_{-0.01} \times 10^{-2}$	$^{+0.19}_{-0.21} \times 10^{-2}$
(0.070,0.100)	$^{+0.29}_{-0.33} \times 10^{-2}$	$^{+0.09}_{-0.09} \times 10^{-2}$	$^{+0.06}_{-0.06} \times 10^{-2}$	$^{+0.00}_{-0.00} \times 10^{-2}$	$^{+0.25}_{-0.29} \times 10^{-2}$
(0.100,0.200)	$^{+0.38}_{-0.73} \times 10^{-2}$	$^{+0.01}_{-0.01} \times 10^{-2}$	$^{+0.07}_{-0.07} \times 10^{-2}$	$^{+0.00}_{-0.00} \times 10^{-2}$	$^{+0.36}_{-0.72} \times 10^{-2}$
(+)chg.					
(-0.200,-0.100)	$^{+0.17}_{-0.17} \times 10^{-2}$	$^{+0.03}_{-0.03} \times 10^{-2}$	$^{+0.11}_{-0.11} \times 10^{-2}$	$^{+0.00}_{-0.00} \times 10^{-2}$	$^{+0.00}_{-0.00} \times 10^{-2}$
(-0.100,-0.070)	$^{+0.19}_{-0.19} \times 10^{-2}$	$^{+0.03}_{-0.03} \times 10^{-2}$	$^{+0.11}_{-0.11} \times 10^{-2}$	$^{+0.00}_{-0.01} \times 10^{-2}$	$^{+0.00}_{-0.00} \times 10^{-2}$
(-0.070,-0.050)	$^{+0.18}_{-0.18} \times 10^{-2}$	$^{+0.00}_{-0.00} \times 10^{-2}$	$^{+0.08}_{-0.08} \times 10^{-2}$	$^{+0.00}_{-0.00} \times 10^{-2}$	$^{+0.00}_{-0.00} \times 10^{-2}$
(-0.050,-0.035)	$^{+0.18}_{-0.18} \times 10^{-2}$	$^{+0.02}_{-0.02} \times 10^{-2}$	$^{+0.07}_{-0.07} \times 10^{-2}$	$^{+0.00}_{-0.00} \times 10^{-2}$	$^{+0.00}_{-0.00} \times 10^{-2}$
(-0.035,0.050)	$^{+0.36}_{-0.41} \times 10^{-2}$	$^{+0.02}_{-0.02} \times 10^{-2}$	$^{+0.18}_{-0.18} \times 10^{-2}$	$^{+0.00}_{-0.00} \times 10^{-2}$	$^{+0.27}_{-0.34} \times 10^{-2}$
(0.050,0.070)	$^{+0.57}_{-0.47} \times 10^{-2}$	$^{+0.03}_{-0.03} \times 10^{-2}$	$^{+0.18}_{-0.18} \times 10^{-2}$	$^{+0.00}_{-0.00} \times 10^{-2}$	$^{+0.51}_{-0.40} \times 10^{-2}$
(0.070,0.100)	$^{+0.53}_{-0.48} \times 10^{-2}$	$^{+0.02}_{-0.02} \times 10^{-2}$	$^{+0.20}_{-0.20} \times 10^{-2}$	$^{+0.00}_{-0.00} \times 10^{-2}$	$^{+0.46}_{-0.40} \times 10^{-2}$
(0.100,0.200)	$^{+0.40}_{-0.46} \times 10^{-2}$	$^{+0.07}_{-0.07} \times 10^{-2}$	$^{+0.15}_{-0.15} \times 10^{-2}$	$^{+0.00}_{-0.00} \times 10^{-2}$	$^{+0.29}_{-0.37} \times 10^{-2}$

Table 11: Systematic uncertainty of unfolded A_N for x_F bin in p+Al

(-)chg.					
x_F	$\delta A_N^{syst.}$	δA_N^{method}	δA_N^{proton}	δA_N^{matrix}	$\delta A_N^{K/\pi}$
(-0.200,-0.100)	$^{+0.37}_{-0.37} \times 10^{-2}$	$^{+0.01}_{-0.01} \times 10^{-2}$	$^{+0.04}_{-0.04} \times 10^{-2}$	$^{+0.00}_{-0.00} \times 10^{-2}$	$^{+0.00}_{-0.00} \times 10^{-2}$
(-0.100,-0.070)	$^{+0.02}_{-0.02} \times 10^{-2}$	$^{+0.01}_{-0.01} \times 10^{-2}$	$^{+0.03}_{-0.03} \times 10^{-2}$	$^{+0.01}_{-0.01} \times 10^{-2}$	$^{+0.00}_{-0.00} \times 10^{-2}$
(-0.070,-0.050)	$^{+0.04}_{-0.04} \times 10^{-2}$	$^{+0.03}_{-0.03} \times 10^{-2}$	$^{+0.03}_{-0.03} \times 10^{-2}$	$^{+0.02}_{-0.01} \times 10^{-2}$	$^{+0.00}_{-0.00} \times 10^{-2}$
(-0.050,-0.035)	$^{+0.06}_{-0.06} \times 10^{-2}$	$^{+0.02}_{-0.02} \times 10^{-2}$	$^{+0.03}_{-0.03} \times 10^{-2}$	$^{+0.03}_{-0.03} \times 10^{-2}$	$^{+0.00}_{-0.00} \times 10^{-2}$
(-0.035,0.050)	$^{+0.19}_{-0.24} \times 10^{-2}$	$^{+0.02}_{-0.02} \times 10^{-2}$	$^{+0.06}_{-0.06} \times 10^{-2}$	$^{+0.03}_{-0.03} \times 10^{-2}$	$^{+0.11}_{-0.19} \times 10^{-2}$
(0.050,0.070)	$^{+0.19}_{-0.21} \times 10^{-2}$	$^{+0.02}_{-0.02} \times 10^{-2}$	$^{+0.06}_{-0.06} \times 10^{-2}$	$^{+0.02}_{-0.02} \times 10^{-2}$	$^{+0.19}_{-0.21} \times 10^{-2}$
(0.070,0.100)	$^{+0.26}_{-0.30} \times 10^{-2}$	$^{+0.09}_{-0.09} \times 10^{-2}$	$^{+0.06}_{-0.06} \times 10^{-2}$	$^{+0.01}_{-0.01} \times 10^{-2}$	$^{+0.25}_{-0.29} \times 10^{-2}$
(0.100,0.200)	$^{+0.36}_{-0.72} \times 10^{-2}$	$^{+0.01}_{-0.01} \times 10^{-2}$	$^{+0.07}_{-0.07} \times 10^{-2}$	$^{+0.00}_{-0.00} \times 10^{-2}$	$^{+0.36}_{-0.72} \times 10^{-2}$
(+)chg.					
x_F	$\delta A_N^{syst.}$	δA_N^{method}	δA_N^{proton}	$\delta A_N^{k/\pi\pm30}$	$\delta A_N^{\mathrm{Unfold}}$
(-0.200,-0.100)	$^{+0.24}_{-0.24} \times 10^{-2}$	$^{+0.03}_{-0.03} \times 10^{-2}$	$^{+0.11}_{-0.11} \times 10^{-2}$	$^{+0.00}_{-0.00} \times 10^{-2}$	$^{+0.00}_{-0.00} \times 10^{-2}$
(-0.100,-0.070)	$^{+0.05}_{-0.05} \times 10^{-2}$	$^{+0.03}_{-0.03} \times 10^{-2}$	$^{+0.11}_{-0.11} \times 10^{-2}$	$^{+0.01}_{-0.01} \times 10^{-2}$	$^{+0.00}_{-0.00} \times 10^{-2}$
(-0.070,-0.050)	$^{+0.03}_{-0.03} \times 10^{-2}$	$^{+0.00}_{-0.00} \times 10^{-2}$	$^{+0.08}_{-0.08} \times 10^{-2}$	$^{+0.01}_{-0.01} \times 10^{-2}$	$^{+0.00}_{-0.00} \times 10^{-2}$
(-0.050,-0.035)	$^{+0.07}_{-0.07} \times 10^{-2}$	$^{+0.02}_{-0.02} \times 10^{-2}$	$^{+0.07}_{-0.07} \times 10^{-2}$	$^{+0.01}_{-0.00} \times 10^{-2}$	$^{+0.00}_{-0.00} \times 10^{-2}$
(-0.035,0.050)	$^{+0.28}_{-0.35} \times 10^{-2}$	$^{+0.02}_{-0.02} \times 10^{-2}$	$^{+0.18}_{-0.18} \times 10^{-2}$	$^{+0.01}_{-0.01} \times 10^{-2}$	$^{+0.27}_{-0.34} \times 10^{-2}$
(0.050,0.070)	$^{+0.51}_{-0.40} \times 10^{-2}$	$^{+0.03}_{-0.03} \times 10^{-2}$	$^{+0.18}_{-0.18} \times 10^{-2}$	$^{+0.01}_{-0.01} \times 10^{-2}$	$^{+0.51}_{-0.40} \times 10^{-2}$
(0.070,0.100)	$^{+0.46}_{-0.40} \times 10^{-2}$	$^{+0.02}_{-0.02} \times 10^{-2}$	$^{+0.20}_{-0.20} \times 10^{-2}$	$^{+0.00}_{-0.01} \times 10^{-2}$	$^{+0.46}_{-0.40} \times 10^{-2}$
(0.100,0.200)	$^{+0.31}_{-0.39} \times 10^{-2}$	$^{+0.07}_{-0.07} \times 10^{-2}$	$^{+0.15}_{-0.15} \times 10^{-2}$	$^{+0.00}_{-0.00} \times 10^{-2}$	$^{+0.29}_{-0.37} \times 10^{-2}$

3.6 Tables of asymmetries with uncertainty

Following tables will list unfolded A_N, statistical uncertainty, and systematic uncertainty for x_F bins.

Table 12: Unfolded A_N with systematic uncertainty for x_F bin in $p + p$

x_F	A_N^{unfold}	$\delta A_N^{stat.}$	$\delta A_N^{syst.}$
(-)chg.			
(-0.200,-0.100)	0.49×10^{-2}	0.55×10^{-2}	$^{+0.10}_{-0.07} \times 10^{-2}$
(-0.100,-0.070)	0.10×10^{-2}	0.39×10^{-2}	$^{+0.04}_{-0.04} \times 10^{-2}$
(-0.070,-0.050)	-0.11×10^{-2}	0.34×10^{-2}	$^{+0.03}_{-0.07} \times 10^{-2}$
(-0.050,-0.035)	-0.30×10^{-2}	0.51×10^{-2}	$^{+0.07}_{-0.15} \times 10^{-2}$
(-0.035,0.050)	0.22×10^{-2}	0.52×10^{-2}	$^{+0.16}_{-0.13} \times 10^{-2}$
(0.050,0.070)	-0.34×10^{-2}	0.34×10^{-2}	$^{+0.18}_{-0.15} \times 10^{-2}$
(0.070,0.100)	-1.52×10^{-2}	0.38×10^{-2}	$^{+0.23}_{-0.45} \times 10^{-2}$
(0.100,0.200)	-0.76×10^{-2}	0.54×10^{-2}	$^{+0.30}_{-0.36} \times 10^{-2}$
(+)chg.			
(-0.200,-0.100)	-0.16×10^{-2}	0.38×10^{-2}	$^{+0.14}_{-0.15} \times 10^{-2}$
(-0.100,-0.070)	0.28×10^{-2}	0.26×10^{-2}	$^{+0.13}_{-0.12} \times 10^{-2}$
(-0.070,-0.050)	0.25×10^{-2}	0.23×10^{-2}	$^{+0.10}_{-0.10} \times 10^{-2}$
(-0.050,-0.035)	0.09×10^{-2}	0.35×10^{-2}	$^{+0.08}_{-0.08} \times 10^{-2}$
(-0.035,0.050)	0.17×10^{-2}	0.35×10^{-2}	$^{+0.34}_{-0.42} \times 10^{-2}$
(0.050,0.070)	0.48×10^{-2}	0.23×10^{-2}	$^{+0.56}_{-0.46} \times 10^{-2}$
(0.070,0.100)	0.70×10^{-2}	0.26×10^{-2}	$^{+0.51}_{-0.50} \times 10^{-2}$
(0.100,0.200)	3.11×10^{-2}	0.37×10^{-2}	$^{+0.37}_{-0.39} \times 10^{-2}$

Table 13: Unfolded A_N with systematic uncertainty for x_F bin in p+Au, centrality range 0-84%.

x_F	A_N^{unfold}	$\delta A_N^{stat.}$	$\delta A_N^{syst.}$
(-)chg.			
(-0.200,-0.100)	0.29×10^{-2}	1.32×10^{-2}	$^{+0.09}_{-0.09} \times 10^{-2}$
(-0.100,-0.070)	0.01×10^{-2}	0.89×10^{-2}	$^{+0.10}_{-0.10} \times 10^{-2}$
(-0.070,-0.050)	-0.77×10^{-2}	0.65×10^{-2}	$^{+0.10}_{-0.10} \times 10^{-2}$
(-0.050,-0.035)	-0.03×10^{-2}	0.73×10^{-2}	$^{+0.10}_{-0.10} \times 10^{-2}$
(-0.035,0.050)	-0.61×10^{-2}	1.53×10^{-2}	$^{+0.17}_{-0.23} \times 10^{-2}$
(0.050,0.070)	-0.91×10^{-2}	0.81×10^{-2}	$^{+0.22}_{-0.24} \times 10^{-2}$
(0.070,0.100)	-0.07×10^{-2}	0.71×10^{-2}	$^{+0.29}_{-0.33} \times 10^{-2}$
(0.100,0.200)	-0.29×10^{-2}	0.81×10^{-2}	$^{+0.38}_{-0.73} \times 10^{-2}$
(+)chg.			
(-0.200,-0.100)	0.74×10^{-2}	0.99×10^{-2}	$^{+0.17}_{-0.17} \times 10^{-2}$
(-0.100,-0.070)	0.78×10^{-2}	0.65×10^{-2}	$^{+0.19}_{-0.19} \times 10^{-2}$
(-0.070,-0.050)	-0.42×10^{-2}	0.50×10^{-2}	$^{+0.18}_{-0.18} \times 10^{-2}$
(-0.050,-0.035)	0.35×10^{-2}	0.56×10^{-2}	$^{+0.18}_{-0.18} \times 10^{-2}$
(-0.035,0.050)	0.19×10^{-2}	0.95×10^{-2}	$^{+0.36}_{-0.41} \times 10^{-2}$
(0.050,0.070)	-0.02×10^{-2}	0.52×10^{-2}	$^{+0.57}_{-0.47} \times 10^{-2}$
(0.070,0.100)	0.76×10^{-2}	0.46×10^{-2}	$^{+0.53}_{-0.48} \times 10^{-2}$
(0.100,0.200)	0.10×10^{-2}	0.56×10^{-2}	$^{+0.40}_{-0.46} \times 10^{-2}$

Table 14: Unfolded A_N with systematic uncertainty for x_F bin in p+Au, centrality range 0-20%.

x_F	A_N^{unfold}	$\delta A_N^{stat.}$	$\delta A_N^{syst.}$
(-)chg.			
(-0.200,-0.100)	2.55×10^{-2}	1.89×10^{-2}	$^{+0.09}_{-0.09} \times 10^{-2}$
(-0.100,-0.070)	-0.35×10^{-2}	1.28×10^{-2}	$^{+0.10}_{-0.10} \times 10^{-2}$
(-0.070,-0.050)	-1.26×10^{-2}	0.94×10^{-2}	$^{+0.10}_{-0.10} \times 10^{-2}$
(-0.050,-0.035)	-0.92×10^{-2}	1.05×10^{-2}	$^{+0.10}_{-0.10} \times 10^{-2}$
(-0.035,0.050)	-2.65×10^{-2}	2.57×10^{-2}	$^{+0.17}_{-0.23} \times 10^{-2}$
(0.050,0.070)	-1.55×10^{-2}	1.39×10^{-2}	$^{+0.22}_{-0.24} \times 10^{-2}$
(0.070,0.100)	-0.81×10^{-2}	1.22×10^{-2}	$^{+0.29}_{-0.33} \times 10^{-2}$
(0.100,0.200)	0.94×10^{-2}	1.40×10^{-2}	$^{+0.38}_{-0.73} \times 10^{-2}$
(+)chg.			
(-0.200,-0.100)	2.26×10^{-2}	1.41×10^{-2}	$^{+0.17}_{-0.17} \times 10^{-2}$
(-0.100,-0.070)	0.35×10^{-2}	0.93×10^{-2}	$^{+0.19}_{-0.19} \times 10^{-2}$
(-0.070,-0.050)	-0.65×10^{-2}	0.71×10^{-2}	$^{+0.18}_{-0.18} \times 10^{-2}$
(-0.050,-0.035)	0.64×10^{-2}	0.80×10^{-2}	$^{+0.18}_{-0.18} \times 10^{-2}$
(-0.035,0.050)	0.64×10^{-2}	1.60×10^{-2}	$^{+0.36}_{-0.41} \times 10^{-2}$
(0.050,0.070)	0.21×10^{-2}	0.89×10^{-2}	$^{+0.57}_{-0.47} \times 10^{-2}$
(0.070,0.100)	0.98×10^{-2}	0.79×10^{-2}	$^{+0.53}_{-0.48} \times 10^{-2}$
(0.100,0.200)	-1.10×10^{-2}	0.96×10^{-2}	$^{+0.40}_{-0.46} \times 10^{-2}$

Table 15: Unfolded A_N with systematic uncertainty for x_F bin in p+Au, centrality range 20-50%

x_F	A_N^{unfold}	$\delta A_N^{stat.}$	$\delta A_N^{syst.}$
(-)chg.			
(-0.200,-0.100)	-3.01×10^{-2}	2.19×10^{-2}	$^{+0.09}_{-0.09} \times 10^{-2}$
(-0.100,-0.070)	0.63×10^{-2}	1.49×10^{-2}	$^{+0.10}_{-0.10} \times 10^{-2}$
(-0.070,-0.050)	0.88×10^{-2}	1.09×10^{-2}	$^{+0.10}_{-0.10} \times 10^{-2}$
(-0.050,-0.035)	0.45×10^{-2}	1.22×10^{-2}	$^{+0.10}_{-0.10} \times 10^{-2}$
(-0.035,0.050)	4.51×10^{-2}	2.44×10^{-2}	$^{+0.17}_{-0.23} \times 10^{-2}$
(0.050,0.070)	-0.44×10^{-2}	1.29×10^{-2}	$^{+0.22}_{-0.24} \times 10^{-2}$
(0.070,0.100)	0.54×10^{-2}	1.12×10^{-2}	$^{+0.29}_{-0.33} \times 10^{-2}$
(0.100,0.200)	-0.01×10^{-2}	1.27×10^{-2}	$^{+0.38}_{-0.73} \times 10^{-2}$
(+)chg.			
(-0.200,-0.100)	-1.71×10^{-2}	1.66×10^{-2}	$^{+0.17}_{-0.17} \times 10^{-2}$
(-0.100,-0.070)	0.32×10^{-2}	1.09×10^{-2}	$^{+0.19}_{-0.19} \times 10^{-2}$
(-0.070,-0.050)	-0.18×10^{-2}	0.83×10^{-2}	$^{+0.18}_{-0.18} \times 10^{-2}$
(-0.050,-0.035)	0.60×10^{-2}	0.95×10^{-2}	$^{+0.18}_{-0.18} \times 10^{-2}$
(-0.035,0.050)	-1.66×10^{-2}	1.52×10^{-2}	$^{+0.36}_{-0.41} \times 10^{-2}$
(0.050,0.070)	0.29×10^{-2}	0.83×10^{-2}	$^{+0.57}_{-0.47} \times 10^{-2}$
(0.070,0.100)	0.11×10^{-2}	0.73×10^{-2}	$^{+0.53}_{-0.48} \times 10^{-2}$
(0.100,0.200)	-0.01×10^{-2}	0.88×10^{-2}	$^{+0.40}_{-0.46} \times 10^{-2}$

Table 16: Unfolded A_N with systematic uncertainty for x_F bin in p+Au, centrality range 50-84%

x_F	A_N^{unfold}	$\delta A_N^{stat.}$	$\delta A_N^{syst.}$
(-)chg.			
(-0.200,-0.100)	1.12×10^{-2}	3.30×10^{-2}	$^{+0.09}_{-0.09} \times 10^{-2}$
(-0.100,-0.070)	0.22×10^{-2}	2.25×10^{-2}	$^{+0.10}_{-0.10} \times 10^{-2}$
(-0.070,-0.050)	-2.95×10^{-2}	1.63×10^{-2}	$^{+0.10}_{-0.10} \times 10^{-2}$
(-0.050,-0.035)	1.73×10^{-2}	1.81×10^{-2}	$^{+0.10}_{-0.10} \times 10^{-2}$
(-0.035,0.050)	-5.17×10^{-2}	3.00×10^{-2}	$^{+0.17}_{-0.23} \times 10^{-2}$
(0.050,0.070)	-0.40×10^{-2}	1.56×10^{-2}	$^{+0.22}_{-0.24} \times 10^{-2}$
(0.070,0.100)	-0.27×10^{-2}	1.36×10^{-2}	$^{+0.29}_{-0.33} \times 10^{-2}$
(0.100,0.200)	-1.91×10^{-2}	1.55×10^{-2}	$^{+0.38}_{-0.73} \times 10^{-2}$
(+)chg.			
(-0.200,-0.100)	1.85×10^{-2}	2.53×10^{-2}	$^{+0.17}_{-0.17} \times 10^{-2}$
(-0.100,-0.070)	3.13×10^{-2}	1.67×10^{-2}	$^{+0.19}_{-0.19} \times 10^{-2}$
(-0.070,-0.050)	-0.35×10^{-2}	1.25×10^{-2}	$^{+0.18}_{-0.18} \times 10^{-2}$
(-0.050,-0.035)	-0.98×10^{-2}	1.42×10^{-2}	$^{+0.18}_{-0.18} \times 10^{-2}$
(-0.035,0.050)	2.80×10^{-2}	1.86×10^{-2}	$^{+0.36}_{-0.41} \times 10^{-2}$
(0.050,0.070)	-1.19×10^{-2}	1.01×10^{-2}	$^{+0.57}_{-0.47} \times 10^{-2}$
(0.070,0.100)	1.35×10^{-2}	0.88×10^{-2}	$^{+0.53}_{-0.48} \times 10^{-2}$
(0.100,0.200)	1.79×10^{-2}	1.07×10^{-2}	$^{+0.40}_{-0.46} \times 10^{-2}$

Table 17: Unfolded A_N with systematic uncertainty for x_F bin in p+Al, centrality range 0-72%

x_F	A_N^{unfold}	$\delta A_N^{stat.}$	$\delta A_N^{syst.}$
(-)chg.			
(-0.200,-0.100)	4.64×10^{-2}	2.23×10^{-2}	$^{+0.37}_{-0.37} \times 10^{-2}$
(-0.100,-0.070)	0.03×10^{-2}	1.50×10^{-2}	$^{+0.02}_{-0.02} \times 10^{-2}$
(-0.070,-0.050)	-0.31×10^{-2}	1.12×10^{-2}	$^{+0.04}_{-0.04} \times 10^{-2}$
(-0.050,-0.035)	1.27×10^{-2}	1.31×10^{-2}	$^{+0.06}_{-0.06} \times 10^{-2}$
(-0.035,0.050)	0.21×10^{-2}	2.17×10^{-2}	$^{+0.19}_{-0.24} \times 10^{-2}$
(0.050,0.070)	-0.96×10^{-2}	1.20×10^{-2}	$^{+0.19}_{-0.21} \times 10^{-2}$
(0.070,0.100)	-0.80×10^{-2}	1.08×10^{-2}	$^{+0.26}_{-0.30} \times 10^{-2}$
(0.100,0.200)	-0.59×10^{-2}	1.28×10^{-2}	$^{+0.36}_{-0.72} \times 10^{-2}$
(+)chg.			
(-0.200,-0.100)	2.26×10^{-2}	1.41×10^{-2}	$^{+0.17}_{-0.17} \times 10^{-2}$
(-0.100,-0.070)	0.35×10^{-2}	0.93×10^{-2}	$^{+0.19}_{-0.19} \times 10^{-2}$
(-0.070,-0.050)	-0.65×10^{-2}	0.71×10^{-2}	$^{+0.18}_{-0.18} \times 10^{-2}$
(-0.050,-0.035)	0.64×10^{-2}	0.80×10^{-2}	$^{+0.18}_{-0.18} \times 10^{-2}$
(-0.035,0.050)	0.64×10^{-2}	1.60×10^{-2}	$^{+0.36}_{-0.41} \times 10^{-2}$
(0.050,0.070)	0.21×10^{-2}	0.89×10^{-2}	$^{+0.57}_{-0.47} \times 10^{-2}$
(0.070,0.100)	0.98×10^{-2}	0.79×10^{-2}	$^{+0.53}_{-0.48} \times 10^{-2}$
(0.100,0.200)	-1.10×10^{-2}	0.96×10^{-2}	$^{+0.40}_{-0.46} \times 10^{-2}$

Table 18: Unfolded A_N with systematic uncertainty for x_F bin in p+Al, centrality range 0-40%

x_F	A_N^{unfold}	$\delta A_N^{stat.}$	$\delta A_N^{syst.}$
(-)chg.			
(-0.200,-0.100)	4.64×10^{-2}	2.23×10^{-2}	$^{+0.37}_{-0.37} \times 10^{-2}$
(-0.100,-0.070)	0.03×10^{-2}	1.50×10^{-2}	$^{+0.02}_{-0.02} \times 10^{-2}$
(-0.070,-0.050)	-0.31×10^{-2}	1.12×10^{-2}	$^{+0.04}_{-0.04} \times 10^{-2}$
(-0.050,-0.035)	1.27×10^{-2}	1.31×10^{-2}	$^{+0.06}_{-0.06} \times 10^{-2}$
(-0.035,0.050)	0.21×10^{-2}	2.17×10^{-2}	$^{+0.19}_{-0.24} \times 10^{-2}$
(0.050,0.070)	-0.96×10^{-2}	1.20×10^{-2}	$^{+0.19}_{-0.21} \times 10^{-2}$
(0.070,0.100)	-0.80×10^{-2}	1.08×10^{-2}	$^{+0.26}_{-0.30} \times 10^{-2}$
(0.100,0.200)	-0.59×10^{-2}	1.28×10^{-2}	$^{+0.36}_{-0.72} \times 10^{-2}$
(+)chg.			
(-0.200,-0.100)	2.26×10^{-2}	1.41×10^{-2}	$^{+0.17}_{-0.17} \times 10^{-2}$
(-0.100,-0.070)	0.35×10^{-2}	0.93×10^{-2}	$^{+0.19}_{-0.19} \times 10^{-2}$
(-0.070,-0.050)	-0.65×10^{-2}	0.71×10^{-2}	$^{+0.18}_{-0.18} \times 10^{-2}$
(-0.050,-0.035)	0.64×10^{-2}	0.80×10^{-2}	$^{+0.18}_{-0.18} \times 10^{-2}$
(-0.035,0.050)	0.64×10^{-2}	1.60×10^{-2}	$^{+0.36}_{-0.41} \times 10^{-2}$
(0.050,0.070)	0.21×10^{-2}	0.89×10^{-2}	$^{+0.57}_{-0.47} \times 10^{-2}$
(0.070,0.100)	0.98×10^{-2}	0.79×10^{-2}	$^{+0.53}_{-0.48} \times 10^{-2}$
(0.100,0.200)	-1.10×10^{-2}	0.96×10^{-2}	$^{+0.40}_{-0.46} \times 10^{-2}$

Table 19: Unfolded A_N with systematic uncertainty for x_F bin in p+Al, centrality range 40-72%

x_F	A_N^{unfold}	$\delta A_N^{stat.}$	$\delta A_N^{syst.}$
(-)chg.			
(-0.200,-0.100)	2.34×10^{-2}	3.96×10^{-2}	$^{+0.37}_{-0.37} \times 10^{-2}$
(-0.100,-0.070)	-0.89×10^{-2}	2.68×10^{-2}	$^{+0.02}_{-0.02} \times 10^{-2}$
(-0.070,-0.050)	-1.01×10^{-2}	2.01×10^{-2}	$^{+0.04}_{-0.04} \times 10^{-2}$
(-0.050,-0.035)	0.81×10^{-2}	2.33×10^{-2}	$^{+0.06}_{-0.06} \times 10^{-2}$
(-0.035,0.050)	-5.28×10^{-2}	3.24×10^{-2}	$^{+0.19}_{-0.24} \times 10^{-2}$
(0.050,0.070)	-0.92×10^{-2}	1.76×10^{-2}	$^{+0.19}_{-0.21} \times 10^{-2}$
(0.070,0.100)	-1.06×10^{-2}	1.58×10^{-2}	$^{+0.26}_{-0.30} \times 10^{-2}$
(0.100,0.200)	0.44×10^{-2}	1.86×10^{-2}	$^{+0.36}_{-0.72} \times 10^{-2}$
(+)chg.			
(-0.200,-0.100)	-1.71×10^{-2}	1.66×10^{-2}	$^{+0.17}_{-0.17} \times 10^{-2}$
(-0.100,-0.070)	0.32×10^{-2}	1.09×10^{-2}	$^{+0.19}_{-0.19} \times 10^{-2}$
(-0.070,-0.050)	-0.18×10^{-2}	0.83×10^{-2}	$^{+0.18}_{-0.18} \times 10^{-2}$
(-0.050,-0.035)	0.60×10^{-2}	0.95×10^{-2}	$^{+0.18}_{-0.18} \times 10^{-2}$
(-0.035,0.050)	-1.66×10^{-2}	1.52×10^{-2}	$^{+0.36}_{-0.41} \times 10^{-2}$
(0.050,0.070)	0.29×10^{-2}	0.83×10^{-2}	$^{+0.57}_{-0.47} \times 10^{-2}$
(0.070,0.100)	0.11×10^{-2}	0.73×10^{-2}	$^{+0.53}_{-0.48} \times 10^{-2}$
(0.100,0.200)	-0.01×10^{-2}	0.88×10^{-2}	$^{+0.40}_{-0.46} \times 10^{-2}$

4 More study to deliver physics message

4.1 A-dependence of A_N of positively charged hadrons at $0.1 < x_F < 0.2$

As A_N of positively charged hadrons shows clear suppression at $0.1 < x_F < 0.2$ in $p + A$ compared with $p + p$, the A-dependence of A_N is studied in this chapter. In recent years, theory papers (Phys.Letter.B 770(2017) 242-251 and others) proposed that measuring A_N in $p + A$ could play a critical role to find the true source of A_N in inclusive hadron production in $p + p$ collision. The fragmentation piece to A_N in $p + A$ collision is proportional to $A^{-1/3}$ while other contributions are expected to make small or no suppression of A_N in $p + A$ collisions. To quantify the effect, fitting the results with A(atomic mass) is suggested to quantify nuclear effect. The study is done in this chapter with additional study using results of centrality classes. For Min-Bias (centrality 0-84% for p+Au, centrality 0-72% for p+Al), the $A^{1/3}$ is used as an axis. The fit function is on the Figure 15.

$$f(A^{1/3}) = \frac{A_N^0}{(A^{1/3})^{\alpha}}, \tag{1}$$

where the α is the power parameter which indicates the nuclear dependence of A_N, scaled onto $A^{1/3}$. A_N^0 is a floating parameter. The systematic uncertainty of α is obtained by checking 1-σ width of of the fit results from 10k samples of Gaussian values which set the center as the central point of the data and the width as the systematic uncertainty, shown in the Figure 16.

If there is no A-dependence, α should be zero while α is expected to be 1.0 for the $A^{1/3}$-dependent case. If the A_N is proportional to the inverse of A, α becomes 3. On the right side of Fig. 15, χ^2 for each power parameter is shown. The range of α is from 0.79 to 2.21 for $\Delta\chi^2 < 1.0$. Even after combining the statistical uncertainty with systematic uncertainty, $\alpha - \Delta\alpha^{total} = 0.72$, far from zero. This supports a statement that a nuclear-dependence exists in A_N in p+A collisions. Moreover, $\Delta\chi^2 = 21$ at $\alpha = 0$ means that the case of NO-nuclear-dependence of A_N is over 4σ away from the result.

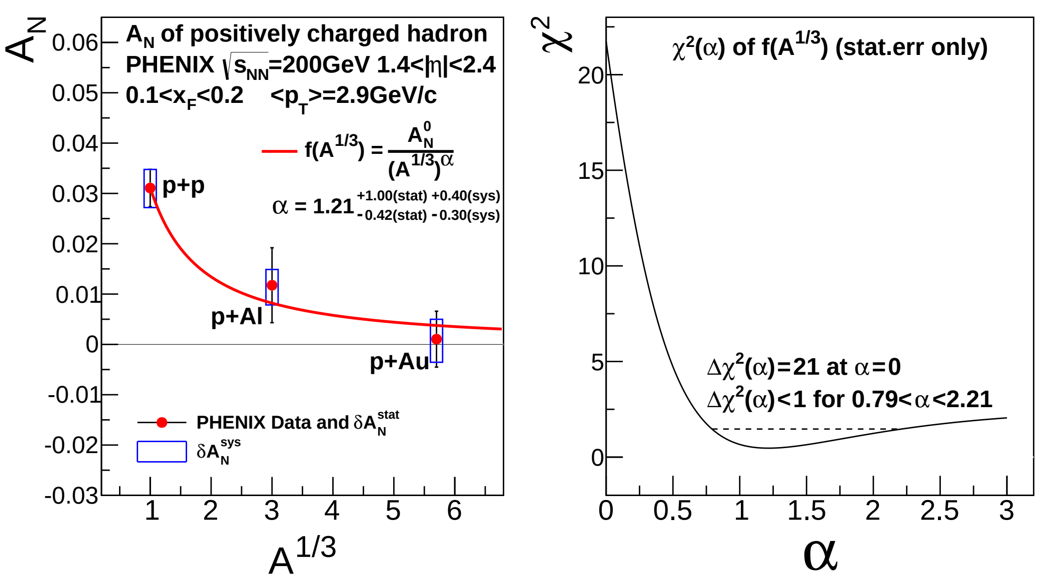

Figure 15: $A^{1/3}$-dependence of A_N of positively charged hadron at $0.1 < x_F < 0.2$ in $p + p$, p+Al, and p+Au collisions

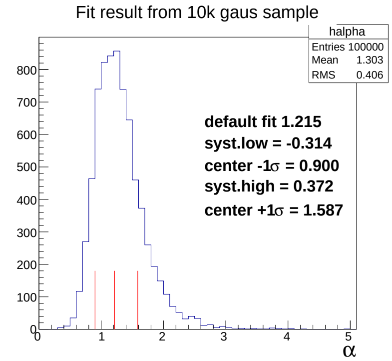

Figure 16: Distribution of the fit results from 10k samples from gaussian distribution which set the center as the central point of the data and the width as the systematic uncertainty of A_N. The width of distribution of α is assigned as systematic uncertainty of α

For the centrality bins, the formula is below:

$$f(N_{coll}^{Avg}) = \frac{A_N^0}{(N_{coll}^{Avg})^{\beta}}. \tag{2}$$

Figure 17 is the fit results for centrality classes 0-20, 20-50, 50-84% in p+Au, and 0-40, 40-84% in p+Al. Averaged-N_{coll} is used as an axis because $< N_{coll} >$ is related to the path length of nuclei in small systems. $< N_{coll} >$ and $\delta < N_{coll} >$ is obtained from PHENIX Ananote 1265, 1290, or calculated from weighted sum of them from the tables if the categorization is different from the tables. Using the same procedure, systematic uncertainty of β is calculated from the width of 10k fit results from a Gaussian distribution where the center is the data points and width is systematic uncertainty of A_N as shown in the Figure 18. In this, 2D-Gaussian is used for including the uncertainty of the uncertainty of N_{coll}. After a test without the uncertainty of N_{coll}, the effect turned out to be very small. The result agrees with the message from the previous pages Fig. 15, β is away from zero.

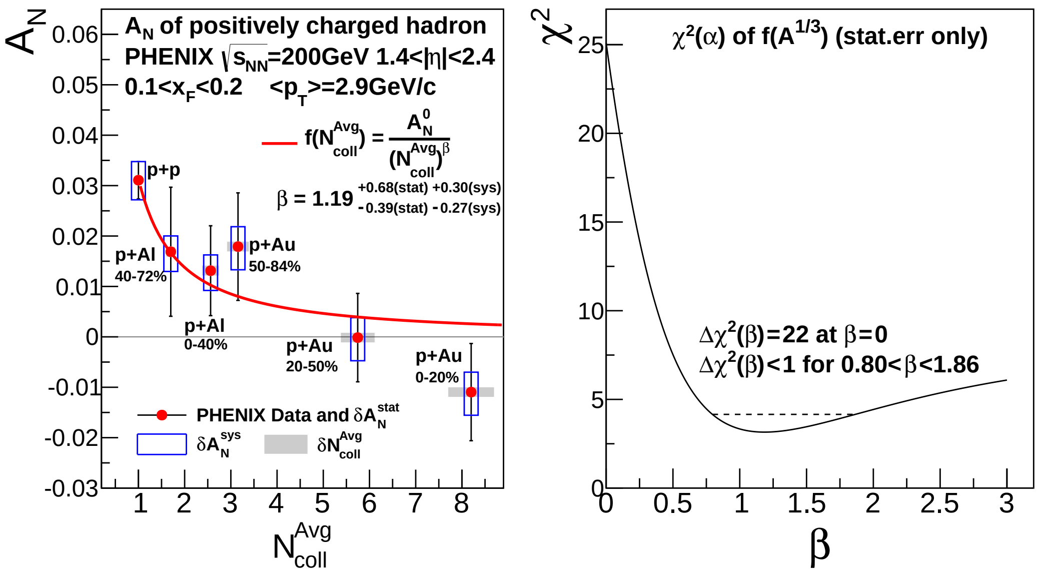

Figure 17: Averaged-N_{coll}-dependence of A_N of positively charged hadron at $0.1 < x_F < 0.2$ for the centrality-categorized results in $p+p$, p+Al, and p+Au collisions

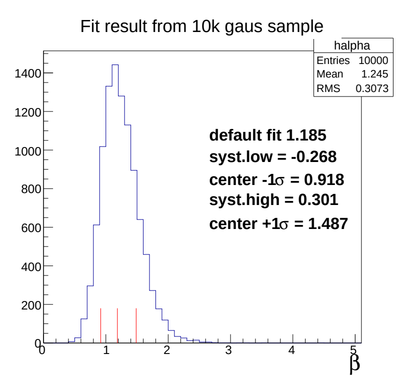

Figure 18: Distribution of the fit result from 10k samples from Gaussian distribution which set the center as the central point of the centrality data and the width as the systematic uncertainty of A_N. The width of distribution of β is assigned as systematic uncertainty of β.

4.2 Comparison of modulations

The nonzero A_N in $p+p$ and suppressed A_N in $p+A$ can be easily recognized when the modulations are compared. The ϕ modulation of positively charged hadron in $p+p$, p+Al, p+Au at $0.1 < x_F < 0.2$ are shown in the Figure 19. The results from Blue, Yellow beams are combined in $p+p$ while only the blue beam was used in p+Al, p+Au. The large statistical uncertainty of a bin is originated from inefficiency of the detector. Modulation in $p+p$ is now showing in $p+A$. δA_N and χ^2/NDF are shown to give an information of the fit.

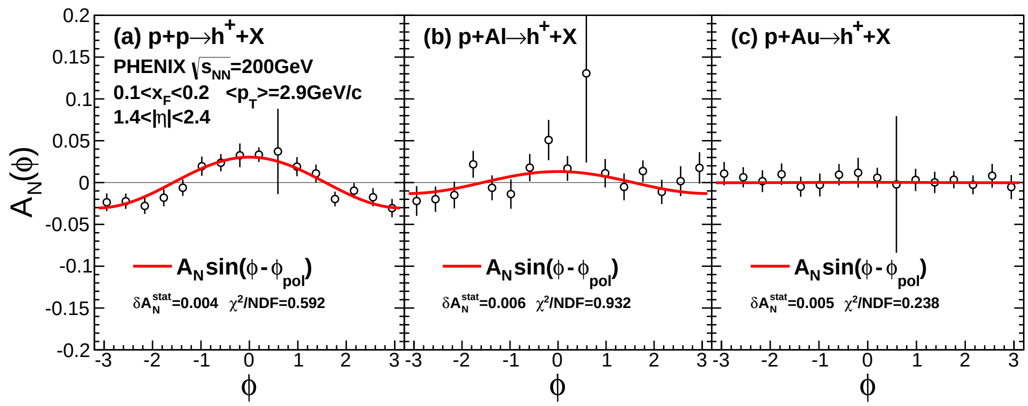

Figure 19: $sin(\phi - \phi_{pol})$ modulation of positively charged hadron in $p+p$, p+Al, p+Au at $0.1 < x_F < 0.2$. The results from Blue, Yellow beams are combined in $p+p$ while only the blue beam was used in p+Al, p+Au. The large statistical uncertainty of a bin is originated from inefficiency of the detector.

Appendix A : Good run list

Good run list for p+Al dataset (North Arm):
436759 436760 436762 436763 436764 436765 436772 436776 436777 436778 436781 436782 436783 436815 436932 436933 436934 436935 436936 436939 437008 437009 437025 437029 437067 437070 437071 437072 437073 437074 437075 437076 437105 437106 437107 437108 437109 437110 437111 437112 437297 437299 437300 437302 437303 437304 437353 437356 437358 437361 437362 437417 437421 437430 437431 437434 437435 437440 437474 437478 437483 437484 437486 437487 437488 437568 437569 437572 437573 437574 437575 437583 437649 437650 437658 437659 437666 437667 437668 437708 437709 437711 437712 437713 437719 437723 437724 437725 437726 437727 437728 437809 437810 437811 437888 437889 437890 437891 437940 437941 437944 438026 438028 438034 438035 438138 438139 438140 438141 438142 438155 438157 438158 438159 438160 438162 438163 438176 438177 438178 438179 438181 438254 438260 438261 438262 438263 438264 438283 438284 438286 438287 438288 438289 438290 438291 438314 438316 438402 438403 438404 438405 438419 438420 438421 438422

Good run list for p+Al dataset (South Arm):
436759 436760 436762 436763 436764 436765 436772 436776 436777 436778 436781 436782 436783 436815 436932 436933 436934 436935 436936 436939 437008 437009 437025 437029 437067 437070 437071 437072 437073 437074 437075 437076 437105 437106 437107 437108 437109 437110 437111 437112 437297 437299 437300 437302 437303 437304 437666 437667 437668 437708 437709 437711 437712 437713 437719 437723 437724 437725 437726 437727 437728 437809 437810 437811 437888 437889 437890 437891 437940 437941 437944 438026 438028 438034 438035 438138 438139 438140 438141 438142 438155 438157 438158 438159 438160 438162 438163 438176 438177 438178 438179 438181 438254 438260 438261 438262 438263 438264 438283 438284 438286 438287 438288 438289 438290 438291 438314 438316 438402 438403 438404 438405 438419 438420 438421 438422